Science Journal of Energy Engineering
2021; 9(4): 79-89
http://www.sciencepublishinggroup.com/j/sjee
doi: 10.11648/j.sjee.20210904.15
ISSN: 2376-810X (Print); ISSN: 2376-8126 (Online)

Short-Circuit Photocurrent Density Determination of Chalcopyrite Solar Cells and Study of Basic Parameters Under AM0, AM1, AM1.5 Spectra

El Hadji Mamadou Keita[1, *], Abdoul Aziz Correa[1], Issa Faye[2], Chamsdine Sow[1], Cheikh Sene[1], Babacar Mbow[1]

[1]Laboratory of Semiconductors and Solar Energy, Physics Department, Faculty of Science and Technology, University Cheikh Anta Diop, Dakar, Senegal

[2]Laboratory of Chemistry and Physics of Materials, University Assane Seck, Ziguinchor, Senegal

Email address:
elouazy@hotmail.fr (El H. M. Keita)

[*]Corresponding author

To cite this article:
El Hadji Mamadou Keita, Abdoul Aziz Correa, Issa Faye, Chamsdine Sow, Cheikh Sene, Babacar Mbow. Short-Circuit Photocurrent Density Determination of Chalcopyrite Solar Cells and Study of Basic Parameters Under AM0, AM1, AM1.5 Spectra. *Science Journal of Energy Engineering*. Vol. 9, No. 4, 2021, pp. 79-89. doi: 10.11648/j.sjee.20210904.15

Received: October 28, 2021; **Accepted**: November 30, 2021; **Published**: December 11, 2021

Abstract: In this work we present a method to evaluate the short-circuit photocurrent density delivered by a solar cell by and study basic parameters which are at the origin of the latter by considering the solar spectra AM0, AM1 and AM1.5. This photocurrent density is the greatest current density that the cell can supply according to the considered parameters for a given illumination. We apply this method to a 4-layer model composed of absorber materials based on chalcopyrite semiconductors ($CuInSe_2$ and $CuInS_2$) and based on a wide band gap window layers (ZnO and CdS) according to the model $ZnO(n^+)/CdS(n)/CuInS_2(p)/CuInSe_2$ (p^+) (model n^+/n /p/p^+). For this model the $CuInS_2$ and $CuInSe_2$ layers are named respectively base and substrate. We exploit continuity equation that governing charge carriers transport in semiconductor materials and use Newton's quadrature integration method over the entire solar spectrum ranging from 1 eV to 4 eV. For this calculation, we have found values of the short-circuit photocurrent density equal to 24.5 $mA.cm^{-2}$, 19.3 $mA.cm^{-2}$, 17.5 $mAcm^{-2}$ respectively for the spectra AM0, AM1 and AM1.5 for the used parameters. The same principle of calculation and reasoning is used to determine and study under a given solar spectrum some intrinsic basic parameters such as the generation rate of carriers, the densities of minority carriers generated and the resulting photocurrents versus the junction depth. The study of these parameters shows a low penetration depth of photons for the considered materials $CuInS_2/CuInSe_2$, losses of charge carriers due to recombination phenomena in surface and interface, bulk recombinations, and losses which are also due to the natural phenomenon of diffusion of carriers in the material under a concentration gradient. This study tries to show that the optimization of the growth conditions of layers, a good choice of material arrangement and a good geometric dimensioning are essential to improve collection efficiency of charge carriers and the short-circuit photocurrent of a photovoltaic cell.

Keywords: Photovoltaic Cell, $CuInS_2/CuInSe_2$, Short-Circuit Photocurrent Density, Intrinsic Parameters

1. Introduction

The performance of a photovoltaic cell depends on its geographical position. To avoid confusion, a standardization has been introduced by defining reference solar spectra. In this work we consider the reference solar spectra AM0, AM1, AM1.5. The photon fluxes $\Phi(\lambda)$ which correspond to these reference irradiance spectra are shown in figure 4.

$CuInSe_2$ and $CuInS_2$ belong to the semiconductor family I-III-VI_2 and are increasingly promising for the mass production of photovoltaic modules. These two materials usually doped p, have quite similar crystalline parameters, band gaps suitable for solar cell operations (in the order of 1.04 eV for $CuInSe_2$ and 1.57 eV for $CuInS_2$). The ZnO and CdS layers are doped n by Al for ZnO and In for CdS, due to their high band gaps they are generally used as window layers

to allow light to pass through in the absorption range of $CuInS_2$ and $CuInSe_2$ [1-10].

In this study $CuInS_2$ is used as a base and $CuInSe_2$ as a substrate. This study inv determining the maximum photocurrent density that the photovoltaic cell can supply according to the considered parameters under a given reference solar spectrum. A second phase consists in studying the profiles of the intrinsic parameters such as the generation rate, the photo-generated minority carrier densities and the resulting photocurrent densities. These intrinsic parameters are at the origin of the spectral response of the cell.

2. Materials and Methods

To determine the theoretical short-circuit photocurrent density and the various intrinsic parameters (generation rate, density of minority carriers and resulting photocurrent densities) under given solar irradiation, we use theoretical calculations based on the continuity equation governing carrier transport in semiconductor materials and the effects of optical absorption coefficient, geometric and electrical parameters of the different materials. It is assumed that the optical reflection coefficient is neglected at each interface in the spectral range used. It is also considered that the space charge region is located only between the n and p regions and there is no electric field outside this region. We neglect recombination phenomena in the space charge region.

On figure 1 we represent the optical absorption coefficients of the different materials and the ZnO reflection coefficient [1, 9, 11].

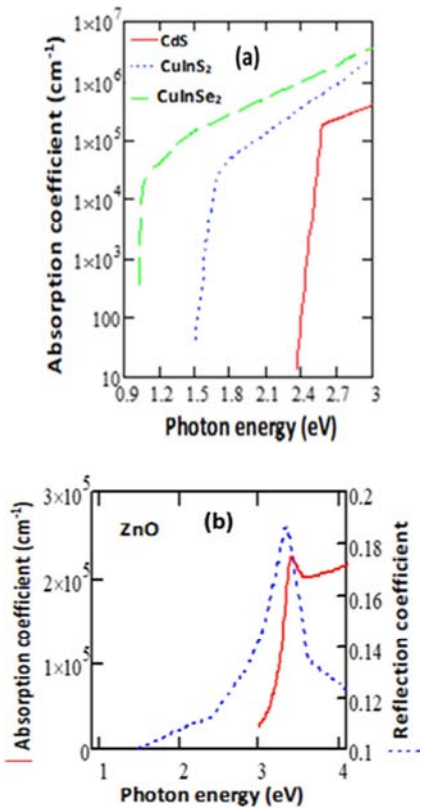

Figure 1. *(a) Absorption coefficient of CdS, $CuInS_2$, $CuInSe_2$ materials versus photon energy [1, 9]; (b) Absorption coefficient and reflection coefficient of ZnO material versus photon energy [11].*

The diagram of the structure is shown on figure 2 and the energy band diagram is represented on figure 3 [4].

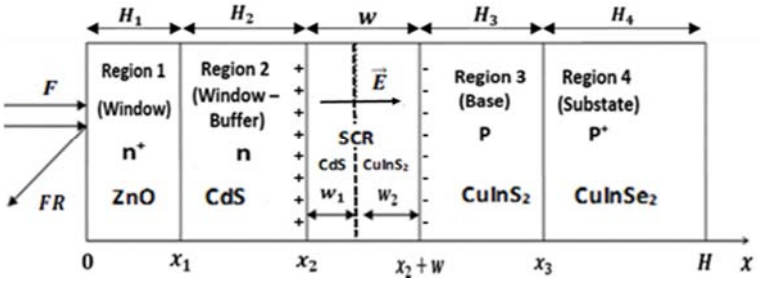

Figure 2. *Diagram of the structure $ZnO(n^+)/CdS(n)/ CuInS_2(p)/CuInSe_2(p^+)$.*

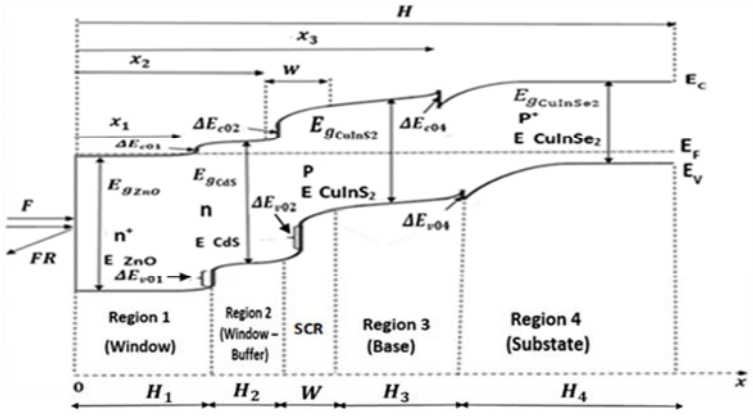

Figure 3. *Energy band diagram of the structure $ZnO(n^+)/CdS(n)CuInS_2(p)/CuInSe_2(p^+)$.*

2.1. Calculation of the Photocurrent in Region 1 (ZnO Layer)

In region 1 (ZnO layer), $0 \leq x \leq x_1$, the photocurrent is essentially due to the holes, the continuity equation is written:

$$\frac{d^2\Delta p_1}{dx^2} - \frac{\Delta p_1}{{L_{p_1}}^2} = \frac{-\alpha_1 F(1-R)e^{-\alpha_1 x}}{D_{p_1}} \tag{1}$$

With

$${L_{p_1}}^2 = D_{p_1}\tau_{p_1} \tag{2}$$

The expression of the generation rate is given by:

$$G_1(x) = \alpha_1 F(1-R)e^{-\alpha_1 x} \tag{3}$$

Boundary conditions are given by previous studies [9, 12]:

$$D_{p_1}\left(\frac{d\Delta p_1}{dx}\right) = S_{p_1}\Delta p_1 \text{ for } x = 0 \tag{4}$$

$$\Delta p_1 = 0 \text{ for } x = x_1 \tag{5}$$

The solution of equation (1) gives the expression of the density of holes in region 1 (ZnO layer), it is written:

$$\Delta p_1(x) = -\frac{\alpha_1 {L_{p_1}}^2 F(1-R)}{D_{p_1}\left(\alpha_1^2 {L_{p_1}}^2 - 1\right)} \cdot \left[e^{-\alpha_1 \cdot x} + \frac{\left(\frac{S_{p_1}L_{p_1}}{D_{p_1}} + \alpha_1 L_{p_1}\right)\cdot \mathrm{sh}\left(\frac{x-H_1}{L_{p_1}}\right) - e^{-\alpha_1 H_1}\left[\frac{S_{p_1}L_{p_1}}{D_{p_1}}\cdot \mathrm{sh}\left(\frac{x}{L_{p_1}}\right) + \mathrm{ch}\left(\frac{x}{L_{p_1}}\right)\right]}{\frac{S_{p_1}L_{p_1}}{D_{p_1}} sh\left(\frac{H_1}{L_{p_1}}\right) + ch\left(\frac{H_1}{L_{p_1}}\right)}\right] \tag{6}$$

The expression of the photocurrent density of holes in region 1 (ZnO layer), is given by:

$$J_{p_1}(\mathrm{x}) = -qD_{p_1}\frac{d\Delta p_1}{dx}$$

it is written as:

$$J_{p_1}(x) = \frac{q\alpha_1 F(1-R)L_{p_1}}{\left(\alpha_1^2 {L_{p_1}}^2 - 1\right)} \times \left\{\frac{\left(\frac{S_{p_1}L_{p_1}}{D_{p_1}} + \alpha_1 L_{p_1}\right) ch\left(\frac{x-H_1}{L_{p_1}}\right) - e^{-\alpha_1 H_1}\left[\frac{S_{p_1}L_{p_1}}{D_{p_1}} ch\left(\frac{x}{L_{p_1}}\right) + sh\left(\frac{x}{L_{p_1}}\right)\right]}{\frac{S_{p_1}L_{p_1}}{D_{p_1}} sh\left(\frac{H_1}{L_{p_1}}\right) + ch\left(\frac{H_1}{L_{p_1}}\right)} - \alpha_1 L_{p_1} e^{-\alpha_1 x}\right\} \tag{7}$$

2.2. Calculation of the Photocurrent in Region 2 (CdS Layer)

In region 2 (CdS layer), $x_1 \leq x \leq x_2$, the photocurrent is also a hole current and results from the contribution of regions 1 and 2 (ZnO and CdS layers). The interface effects are characterized by a recombination velocity at the interface noted S_{p_2}. The continuity equation is given by:

$$\frac{d^2\Delta p_2}{dx^2} - \frac{\Delta p_2}{{L_{p_2}}^2} = \frac{-\alpha_2 F(1-R)e^{-\alpha_1 H_1}e^{-\alpha_2(x-H_1)}}{D_{p_2}} \tag{8}$$

With

$${L_{p_2}}^2 = D_{p_2}\tau_{p_2} \tag{9}$$

The expression of the generation rate is given by:

$$G_2(x) = \alpha_2 F(1-R)e^{-\alpha_1 H_1}e^{-\alpha_2(x-H_1)} \tag{10}$$

Boundary conditions are given by previous studies [12-14]:

$$D_{p_2}\frac{d\Delta p_2}{dx} = S_{p_2}\Delta p_2 + D_{p_1}\frac{d\Delta p_1}{dx} \text{ for } x = x_1 \tag{11}$$

$$\Delta p_2 = 0 \text{ for } x = x_2 \tag{12}$$

The solution of equation (8) gives the density of photo-created holes in region 2 (CdS layer), it is given by:

$$\Delta p_2(x) = -\frac{\alpha_2 {L_{p_2}}^2 F(1-R)\, e^{-\alpha_1 H_1}}{D_{p_2}\left({\alpha_2}^2 {L_{p_2}}^2 - 1\right)} \cdot \left[e^{-\alpha_2 (x-H_1)} + \frac{\left(\frac{S_{p_2} L_{p_2}}{D_{p_2}} + \alpha_2 L_{p_2}\right) \cdot \mathrm{sh}\left(\frac{x-(H_1+H_2)}{L_{p_2}}\right)}{\frac{S_{p_2} L_{p_2}}{D_{p_2}} sh\left(\frac{H_2}{L_{p_2}}\right) + ch\left(\frac{H_2}{L_{p_2}}\right)} - \frac{e^{-\alpha_2 H_2}\left[\frac{S_{p_2} L_{p_2}}{D_{p_2}} \cdot \mathrm{sh}\left(\frac{x-H_1}{L_{P_2}}\right) + \mathrm{ch}\left(\frac{x-H_1}{L_{p_2}}\right)\right]}{\frac{S_{p_2} L_{p_2}}{D_{p_2}} sh\left(\frac{H_2}{L_{p_2}}\right) + ch\left(\frac{H_2}{L_{p_2}}\right)} \right] -$$

$$\frac{\mathrm{sh}\left(\frac{x-(H_1+H_2)}{L_{p_2}}\right) \cdot \alpha_1 F(1-R) L_{p_1} L_{p_2}}{D_{p_2}\left(\alpha_1^2 {L_{p_1}}^2 - 1\right)\left\{\frac{S_{p_2} L_{p_2}}{D_{p_2}} sh\left(\frac{H_2}{L_{p_2}}\right) + ch\left(\frac{H_2}{L_{p_2}}\right)\right\}} \times \left\{ \frac{\left(\frac{S_{p_1} L_{p_1}}{D_{p_1}} + \alpha_1 L_{p_1}\right) - e^{-\alpha_1 H_1}\left[\frac{S_{p_1} L_{p_1}}{D_{p_1}} ch\left(\frac{H_1}{L_{p_1}}\right) + sh\left(\frac{H_1}{L_{p_1}}\right)\right]}{\frac{S_{p_1} L_{p_1}}{D_{p_1}} sh\left(\frac{H_1}{L_{p_1}}\right) + ch\left(\frac{H_1}{L_{p_1}}\right)} - \alpha_1 L_{p_1} e^{-\alpha_1 H_1} \right\} \quad (13)$$

The expression of the resulting photocurrent density of holes in region 2 (CdS) is given by:

$$J_{p_2}(\mathrm{x}) = -qD_{p_2} \frac{d\Delta p_2}{dx},$$

it is written as:

$$J_{p_2}(\mathrm{x}) = \frac{q\alpha_2 F(1-R) L_{p_2} e^{-\alpha_1 H_1}}{\left({\alpha_2}^2 {L_{p_2}}^2 - 1\right)} \left\{ \frac{\left(\frac{S_{p_2} L_{p_2}}{D_{p_2}} + \alpha_2 L_{p_2}\right) \mathrm{ch}\left(\frac{x-(H_1+H_2)}{L_{p_2}}\right)}{\frac{S_{p_2} L_{p_2}}{D_{p_2}} sh\left(\frac{H_2}{L_{p_2}}\right) + ch\left(\frac{H_2}{L_{p_2}}\right)} - \frac{e^{-\alpha_2 H_2}\left[\frac{S_{p_2} L_{p_2}}{D_{p_2}} ch\left(\frac{x-H_1}{L_{p_2}}\right) + sh\left(\frac{x-H_1}{L_{p_2}}\right)\right]}{\frac{S_{p_2} L_{p_2}}{D_{p_2}} sh\left(\frac{H_2}{L_{p_2}}\right) + ch\left(\frac{H_2}{L_{p_2}}\right)} - \alpha_2 L_{p_2} e^{-\alpha_2 (x-H_1)} \right\} +$$

$$\frac{\mathrm{ch}\left(\frac{x-(H_1+H_2)}{L_{p_2}}\right) q\alpha_1 F(1-R) L_{p_1}}{\left(\alpha_1^2 {L_{p_1}}^2 - 1\right)\left[\frac{S_{p_2} L_{p_2}}{D_{p_2}} sh\left(\frac{H_2}{L_{p_2}}\right) + ch\left(\frac{H_2}{L_{p_2}}\right)\right]} \times \left\{ \frac{\left(\frac{S_{p_1} L_{p_1}}{D_{p_1}} + \alpha_1 L_{p_1}\right) - e^{-\alpha_1 H_1}\left[\frac{S_{p_1} L_{p_1}}{D_{p_1}} ch\left(\frac{H_1}{L_{p_1}}\right) + sh\left(\frac{H_1}{L_{p_1}}\right)\right]}{\frac{S_{p_1} L_{p_1}}{D_{p_1}} sh\left(\frac{H_1}{L_{p_1}}\right) + ch\left(\frac{H_1}{L_{p_1}}\right)} - \alpha_1 L_{p_1} e^{-\alpha_1 H_1} \right\} \quad (14)$$

2.3. Calculation of the Photocurrent in the Space Charge Region

In the space charge region, the recombinations of carriers are neglected. It is formed by two areas: In the first area $x_2 \leq x \leq x_2 + w_1$, the thickness is fixed at w_1 (CdS), the continuity equation for the photo-created holes is written as:

$$-\frac{1}{q}\frac{dJ_{w_1}}{dx} + \alpha_2 F(1-R) e^{-\alpha_1 H_1} e^{-\alpha_2 (x-H_1)} = 0 \quad (15)$$

With

$$J_{w_1}(x_2) = 0 \quad (16)$$

The photocurrent density of holes in this first area (CdS), is given by the solution of equation (15), it is written as:

$$J_{w_1}(x) = -qF(1-R) e^{-\alpha_1 \cdot H_1} \times \left[e^{-\alpha_2 (x-H_1)} - e^{-\alpha_2 \cdot H_2} \right] \quad (17)$$

In the second area $x_2 + w_1 \leq x \leq x_2 + w_1 + w_2$, the thickness is fixed at w_2 ($CuInS_2$), the continuity equation for the photo-created holes is written as:

$$-\frac{1}{q}\frac{dJ_{w_2}}{dx} + \alpha_3 F(1-R) e^{-\alpha_1 H_1} e^{-\alpha_2 (H_2+w_1)} \times e^{-\alpha_3 [x-(H_1+H_2+w_1)]} = 0 \quad (18)$$

With

$$J_{w_2}(x_2 + w_1) = 0 \quad (19)$$

The photocurrent density of holes in this second area ($CuInS_2$), is given by the solution of equation (18), it is written as:

$$J_{w_2}(x) = -qF(1-R) e^{-\alpha_1 H_1} e^{-\alpha_2 (H_2+w_1)} \times \left[e^{-\alpha_3 [x-(H_1+H_2+w_1)]} - 1 \right] \quad (20)$$

2.4. Calculation of the Photocurrent in the Substrate (Region 4)

In region 4, the substrate ($CuInSe_2$), the photocurrent is due to the photo-created electrons, the continuity equation is given by:

$$\frac{d^2 \Delta n_4}{dx^2} - \frac{\Delta n_4}{L_{n_4}^2} = \frac{-\alpha_4}{D_{n_4}} F(1-R) e^{-\alpha_1 H_1} e^{-\alpha_2 (H_2+w_1)} \times e^{-\alpha_3 (H_3+w_2)} e^{-\alpha_4 [x-(H-H_4)]} \quad (21)$$

The expression of the generation rate is given by:

$$G_4(x) = \alpha_4 F(1-R) e^{-\alpha_1 H_1} e^{-\alpha_2 (H_2+w_1)} \times e^{-\alpha_3 (H_3+w_2)} e^{-\alpha_4 [x-(H-H_4)]} \quad (22)$$

Boundary conditions are given by previous studies [9, 12]:

$$D_{n_4} \frac{d\Delta n_4}{dx} = -S_{n_4} \Delta n_4 \text{ for } x = H \quad (23)$$

$$\Delta n_4 = 0 \text{ for } x = x_3 \tag{24}$$

The density of photo-created electrons in region 4 (substrate: $CuInSe_2$) is solution of equation (21), It is given by:

$$\Delta n_4(x) = -\frac{\alpha_4 {L_{n_4}}^2 F(1-R)\, e^{[(\alpha_2-\alpha_1)H_1]}}{D_{n_4}\left(\alpha_4^2 {L_{n_4}}^2 - 1\right)} \times e^{[(\alpha_3-\alpha_2)(H_1+H_2+w_1)]} e^{[(\alpha_4-\alpha_3)(H-H_4)]} \times \left[e^{-\alpha_4 x} + \frac{\left(\alpha_4 L_{n_4} - \frac{S_{n_4}L_{n_4}}{D_{n_4}}\right) e^{-\alpha_4 H} \cdot \mathrm{sh}\left(\frac{x-(H-H_4)}{L_{n_4}}\right)}{\frac{S_{n_4}L_{n_4}}{D_{n_4}} sh\left(\frac{H_4}{L_{n_4}}\right) + ch\left(\frac{H_4}{L_{n_4}}\right)} - \frac{e^{-\alpha_4(H-H_4)}\left[\frac{S_{n_4}L_{n_4}}{D_{n_4}} \cdot \mathrm{sh}\left(\frac{H-x}{L_{n_4}}\right) + \mathrm{ch}\left(\frac{H-x}{L_{n_4}}\right)\right]}{\frac{S_{n_4}L_{n_4}}{D_{n_4}} sh\left(\frac{H_4}{L_{n_4}}\right) + ch\left(\frac{H_4}{L_{n_4}}\right)} \right] \tag{25}$$

The resulting photocurrent density of electrons in region 4 (substrate: $CuInSe_2$) is given by:

$$J_{n_4}(\mathrm{x}) = qD_{n_4}\frac{d\Delta n_4}{dx}$$

it is written as:

$$J_{n_4}(\mathrm{x}) = -\frac{q\,\alpha_4 L_{n_4} F(1-R)\, e^{[(\alpha_2-\alpha_1)H_1]}\, e^{[(\alpha_3-\alpha_2)(H_1+H_2+w_1)]}}{\left(\alpha_4^2 {L_{n_4}}^2 - 1\right)} \times e^{[(\alpha_4-\alpha_3)(H-H_4)]} \times \left[\frac{\left(\alpha_4 L_{n_4} - \frac{S_{n_4}L_{n_4}}{D_{n_4}}\right) e^{-\alpha_4 H} \cdot \mathrm{ch}\left(\frac{x-(H-H_4)}{L_{n_4}}\right)}{\frac{S_{n_4}L_{n_4}}{D_{n_4}} sh\left(\frac{H_4}{L_{n_4}}\right) + ch\left(\frac{H_4}{L_{n_4}}\right)} + \frac{e^{-\alpha_4(H-H_4)}\left[\frac{S_{n_4}L_{n_4}}{D_{n_4}} \cdot \mathrm{ch}\left(\frac{H-x}{L_{n_4}}\right) + \mathrm{sh}\left(\frac{H-x}{L_{n_4}}\right)\right]}{\frac{S_{n_4}L_{n_4}}{D_{n_4}} sh\left(\frac{H_4}{L_{n_4}}\right) + ch\left(\frac{H_4}{L_{n_4}}\right)} - \alpha_4 L_{n_4} e^{-\alpha_4 x} \right] \tag{26}$$

2.5. Calculation of the Photocurrent in the Base (Region 3)

In region 3, the base ($CuInS_2$ layer), $x_2 + w \le x \le x_3$, the photocurrent is also due to the photo-created electrons, it results from the contribution of the base itself and the substrate. The continuity equation is given by:

$$\frac{d^2\Delta n_3}{dx^2} - \frac{\Delta n_3}{L_{n_3}^2} = \frac{-\alpha_3}{D_{n_3}} F(1-R) e^{-\alpha_1 H_1} e^{-\alpha_2(H_2+w_1)} \times e^{-\alpha_3[x-(H_1+H_2+w_1)]} \tag{27}$$

The expression of the generation rate is given by:

$$G_3(x) = \alpha_3 F(1-R) e^{-\alpha_1 H_1} e^{-\alpha_2(H_2+w_1)} \times e^{-\alpha_3[x-(H_1+H_2+w_1)]} \tag{28}$$

Boundary conditions can be written using previous studies [4]:

$$\Delta n_3 = 0 \text{ for } x = x_2 + w \tag{29}$$

$$D_{n_3}\frac{d\Delta n_3}{dx} = -S_{n_3}\Delta n_3 + D_{n_4}\frac{d\Delta n_4}{dx} \text{ for } x = x_3 \tag{30}$$

The density of photo-created electrons in region 3 (base: $CuInS_2$), is solution of equation (27), it is given by:

$$\Delta n_3(x) = -\frac{\alpha_3 {L_{n_3}}^2 F(1-R)\, e^{[(\alpha_2-\alpha_1)H_1]}\, e^{[(\alpha_3-\alpha_2)(H_1+H_2+w_1)]}}{D_{n_3}\left(\alpha_3^2 {L_{n_3}}^2 - 1\right)} \times \left[e^{-\alpha_3 x} + \frac{\left(\alpha_3 L_{n_3} - \frac{S_{n_3}L_{n_3}}{D_{n_3}}\right) e^{-\alpha_3(H-H_4)} \cdot \mathrm{sh}\left[\frac{x-(H_1+H_2+w)}{L_{n_3}}\right]}{\frac{S_{n_3}L_{n_3}}{D_{n_3}} sh\left[\frac{H_3}{L_{n_3}}\right] + ch\left[\frac{H_3}{L_{n_3}}\right]} - \frac{e^{-\alpha_3(H_1+H_2+w)}\left[\frac{S_{n_3}L_{n_3}}{D_{n_3}} \cdot \mathrm{sh}\left(\frac{(H-H_4)-x}{L_{n_3}}\right) + \mathrm{ch}\left(\frac{(H-H_4)-x}{L_{n_3}}\right)\right]}{\frac{S_{n_3}L_{n_3}}{D_{n_3}} sh\left[\frac{H_3}{L_{n_3}}\right] + ch\left[\frac{H_3}{L_{n_3}}\right]} \right] - \frac{\mathrm{sh}\left[\frac{x-(H_1+H_2+w)}{L_{n_3}}\right] \alpha_4 L_{n_4} L_{n_3} F(1-R)\, e^{[(\alpha_2-\alpha_1)H_1]}}{D_{n_3}\left(\alpha_4^2 {L_{n_4}}^2 - 1\right)\left\{\frac{S_{n_3}L_{n_3}}{D_{n_3}} sh\left[\frac{H_3}{L_{n_3}}\right] + ch\left[\frac{H_3}{L_{n_3}}\right]\right\}} \times$$

$$e^{[(\alpha_3-\alpha_2)(H_1+H_2+w_1)]} e^{[(\alpha_4-\alpha_3)(H-H_4)]} \times \left[\frac{\left(\alpha_4 L_{n_4} - \frac{S_{n_4}L_{n_4}}{D_{n_4}}\right) e^{-\alpha_4 H}}{\frac{S_{n_4}L_{n_4}}{D_{n_4}} sh\left(\frac{H_4}{L_{n_4}}\right) + ch\left(\frac{H_4}{L_{n_4}}\right)} + \frac{e^{-\alpha_4(H-H_4)}\left[\frac{S_{n_4}L_{n_4}}{D_{n_4}} \mathrm{ch}\left(\frac{H_4}{L_{n_4}}\right) + \mathrm{sh}\left(\frac{H_4}{L_{n_4}}\right)\right]}{\frac{S_{n_4}L_{n_4}}{D_{n_4}} sh\left(\frac{H_4}{L_{n_4}}\right) + ch\left(\frac{H_4}{L_{n_4}}\right)} - \alpha_4 L_{n_4} e^{-\alpha_4(H-H_4)} \right] \tag{31}$$

The expression of the photocurrent density of electrons in region 3 (base: $CuInS_2$) is given by:

$$J_{n_3}(\mathrm{x}) = qD_{n_3}\frac{d\Delta n_3}{dx},$$

it is written as:

$$J_{n_3}(\mathrm{x}) = -\frac{q\,\alpha_3\,L_{n_3}F(1-R)\,e^{[(\alpha_2-\alpha_1)H_1]}\,e^{[(\alpha_3-\alpha_2)(H_1+H_2+w_1)]}}{(\alpha_3{}^2L_{n_3}{}^2-1)} \times \left[\frac{\left(\alpha_3L_{n_3}-\frac{S_{n_3}L_{n_3}}{D_{n_3}}\right)e^{-\alpha_3(H-H_4)}\cdot\mathrm{ch}\left[\frac{x-(H_1+H_2+w)}{L_{n_3}}\right]}{\frac{S_{n_3}L_{n_3}}{D_{n_3}}sh\left[\frac{H_3}{L_{n_3}}\right]+ch\left[\frac{H_3}{L_{n_3}}\right]}+\frac{e^{-\alpha_3(H_1+H_2+w)}\left[\frac{S_{n_3}L_{n_3}}{D_{n_3}}\cdot\mathrm{ch}\left(\frac{(H-H_4)-x}{L_{n_3}}\right)+\mathrm{sh}\left(\frac{(H-H_4)-x}{L_{n_3}}\right)\right]}{\frac{S_{n_3}L_{n_3}}{D_{n_3}}sh\left[\frac{H_3}{L_{n_3}}\right]+ch\left[\frac{H_3}{L_{n_3}}\right]}-\alpha_3L_{n_3}e^{-\alpha_3x}\right] - \frac{\mathrm{ch}\left[\frac{x-(H_1+H_2+w)}{L_{n_3}}\right]\,q\,\alpha_4\,L_{n_4}F(1-R)\,e^{[(\alpha_2-\alpha_1)H_1]}}{(\alpha_4{}^2L_{n_4}{}^2-1)\left\{\frac{S_{n_3}L_{n_3}}{D_{n_3}}sh\left[\frac{H_3}{L_{n_3}}\right]+ch\left[\frac{H_3}{L_{n_3}}\right]\right\}} \times e^{[(\alpha_3-\alpha_2)(H_1+H_2+w_1)]}e^{[(\alpha_4-\alpha_3)(H-H_4)]} \times \left[\frac{\left(\alpha_4L_{n_4}-\frac{S_{n_4}L_{n_4}}{D_{n_4}}\right)e^{-\alpha_4H}}{\frac{S_{n_4}L_{n_4}}{D_{n_4}}sh\left(\frac{H_4}{L_{n_4}}\right)+ch\left(\frac{H_4}{L_{n_4}}\right)}+\frac{e^{-\alpha_4(H-H_4)}\left[\frac{S_{n_4}L_{n_4}}{D_{n_4}}\mathrm{ch}\left(\frac{H_4}{L_{n_4}}\right)+\mathrm{sh}\left(\frac{H_4}{L_{n_4}}\right)\right]}{\frac{S_{n_4}L_{n_4}}{D_{n_4}}sh\left(\frac{H_4}{L_{n_4}}\right)+ch\left(\frac{H_4}{L_{n_4}}\right)}-\alpha_4L_{n_4}e^{-\alpha_4(H-H_4)}\right] \quad (32)$$

2.6. Calculation of the Total Photocurrent

Carriers which reach the space charge region are assumed to be collected. The total photocurrent collected is the sum of the photocurrents of the different regions, that pass through the space charge region, it is given by the following equation:

$$J_{ph} = J_{p_2}(\mathrm{x}_2) + J_{w_1}(x_2 + w_1) + J_{w_2}(x_2 + w) + J_{n_3}(x_2 + w) \quad (33)$$

3. Results and Discussion

3.1. Short-Circuit Photocurrent Density

In figure 4 we represent the photon fluxes which correspond to the three reference solar spectra AM0, AM1, AM1.5 versus the wavelength, they are adapted from [15]. It is noted $\Phi(\lambda)$ and is expressed in $cm^{-2}.s^{-1}.\mu m^{-1}$.

In figure 5 we represent the photon fluxes versus the photon energy, it is noted $F(E)$ and is expressed in $cm^{-2}.s^{-1}.eV^{-1}$. The relation between $\Phi(\lambda)$ and $F(E)$ is given by the equations 34 and 35. The wavelength λ is expressed in μm and the energy E in is expressed in eV.

$$\lambda\,(\mu m) = \frac{1.24}{E\,(eV)} \quad (34)$$

$$F\,(E) = \Phi(\lambda) \times \frac{1.24}{E^2} \quad (35)$$

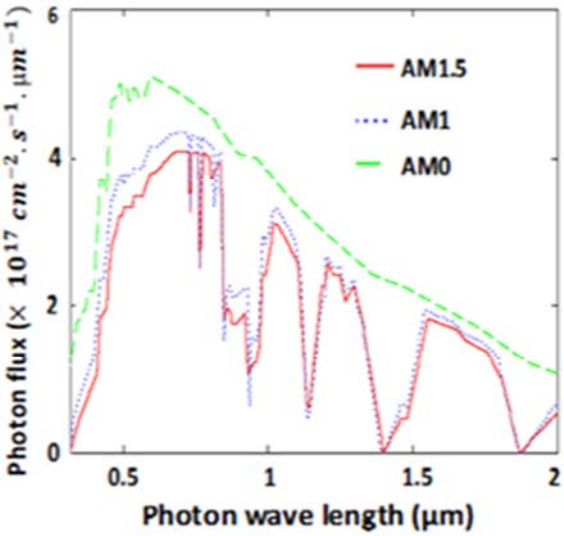

Figure 4. *Photon flux vs. photon wave length [15].*

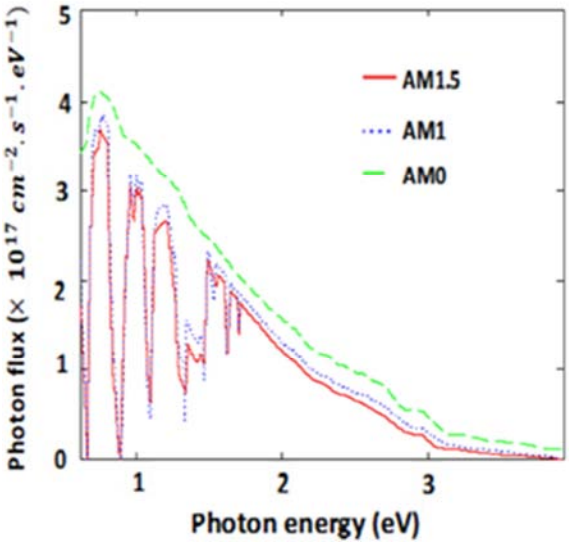

Figure 5. *Photon flux vs. photon energy.*

For this study, the following parameters are considered, these parameters characterize the electrical, geometric and structural properties of the layers:

Region 1: $Sp_1=2.10^7$ $cm.s^{-1}$; $H_1=0.3$ µm; $Lp_1=0.4$ µm; $Dp_1=0.51$ $cm^2.s^{-1}$;

Region 2: $Sp_2=2.10^5$ $cm.s^{-1}$; $H_2=0.1$ µm; $Lp_2=0.5$ µm; $Dp_2=0.64$ $cm^2.s^{-1}$;

Region 3: $Ln_3=3$ µm; $H_3=1$ µm; $Sn_3=2.10^5$ $cm.s^{-1}$; $Dn_3=5.13$ $cm^2.s^{-1}$;

Region 4: $Sn_4=2.10^7$ $cm.s^{-1}$; $Ln_4=1$ µm; $H_4=98.5$ µm; $Dn_4=10.27$ $cm^2.s^{-1}$;

Space charge region: $w_1=0.02$ µm; $w_2=0.08$ µm; W=0.1 µm;

Structure thickness: H=100 µm

In figure 6 we represent, under the spectra AM0, AM1 and AM1.5, the resulting photocurrent density $J_{ph}(E)$ versus photon energy. It is expressed in $A.cm^{-2}.eV^{-1}$. To draw this graph we have used the relations 33 and 35.

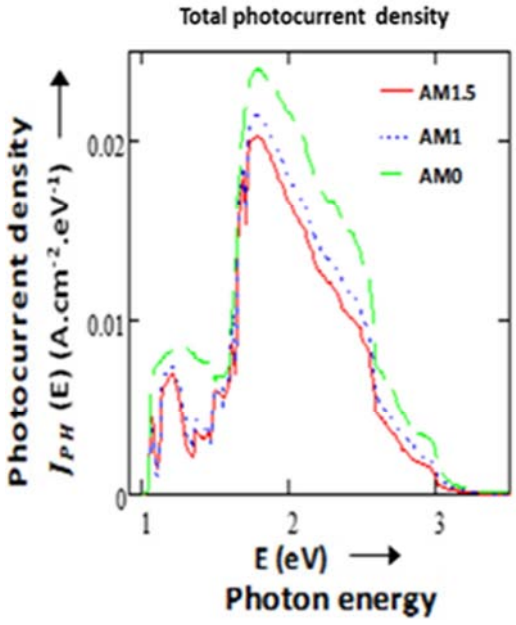

Figure 6. *Resulting photocurrent density vs. photon energy under polychromatic illumination (AM0, AM1, AM1.5 solar spectra).*

Figure 7 shows the contribution of each region of the photovoltaic structure on the resulting photocurrent density for AM1.5 spectrum. This graph shows that the response of the cell on the spectrum depends essentially on the layers of $CuInSe_2$ and of $CuInS_2$. This response therefore depends on the space charge region, the base ($CuInS_2$) and the substrate ($CuInSe_2$). However despite that the photon flux is higher in the absorption range of the substrate (1.04 eV < E < 1.57 eV) we notice that the contribution of the substrate is lower than those of the base and the space charge region (1.57 eV < E < 2 eV), this is due to losses of carriers at the interface base-substrate (the recombination velocity is fixed at $Sn_3 = 2.10^5\ cm.s^{-1}$) and losses of carriers in bulk. So the state of the interface plays an important role in the collection of charge carriers. However the drop in current density beyond 2 eV is due to the decrease in photon flux and the absorption of photons by the CdS layer.

Since absorption coefficients and photon fluxes depend on energy, the short-circuit photocurrent J_{sc} is obtained by integrating the photocurrent density $J_{ph}(E)$ over the entire solar spectrum (from 1 eV to 4). The short-circuit photocurrent density expression is written using Newton's quadrature:

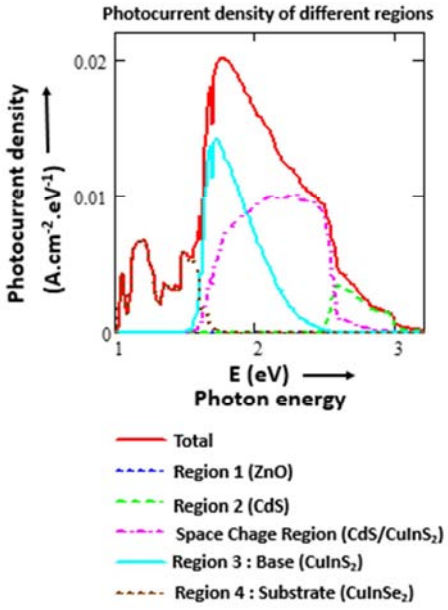

Figure 7. *Photocurrent density of different regions vs. photon energy under polychromatic illumination (AM1.5 solar spectrum).*

$$J_{sc} = \int_1^4 J_{ph}(E)dE \approx \frac{\delta E}{2}\left[J_{ph}(E_1) + J_{ph}(E_{m+1}) + 2\sum_{i=2}^{m} J_{ph}(E_i)\right] \quad (36)$$

With: $E \in [1,4]$; $E_1 = 1\ eV$; $E_{m+1} = 4$; $\delta E = \frac{E_{m+1} - E_1}{m}$

$$E_{i+1} = E_1 + i \cdot \delta E \text{ with: } i: 1 \ldots m$$

For this calculation, we pose m=100

For the considered parameters in table 1, we obtain the short-circuit photocurrent density established in table 2 for the three solar spectra AM0, AM1, AM1.5. This photocurrent is constant throughout the photovoltaic structure and is expressed in A.cm^{-2}. Figure 8 shows the evolution of this photocurrent versus the junction depht for each spectrum.

Table 1. *Physical parameters considered.*

Region i	H_i(µm)	L_{p_i}, L_{n_i}(µm)	$S_{p_i}, S_{n_i}(cm.s^{-1})$	$\mu_{p_i}, \mu_{n_i}(cm^2/V.s)$	$D_{p_i}, D_{n_i}(cm^2.s^{-1})$
ZnO (R 1)	0.3	0.3	2×10^7	20	0.51
CdS (R 2)	0.1	0.4	2×10^5	25	0.64
$CuInS_2$ (R 3)	1	3	2×10^5	200	5.13
$CuInSe_2$ (R 4)	98.5	1	2×10^7	400	10.27

Table 2. *Short-circuit photocurrent density.*

Solar spectrum	AM0	AM1	AM1.5
Short-circuit photocurrent density	24.52 mA.cm^{-2}	19.30 mA.cm^{-2}	17.50 mA.cm^{-2}

These values obtained from Table 2 are well within the range of values published in the literature [1].

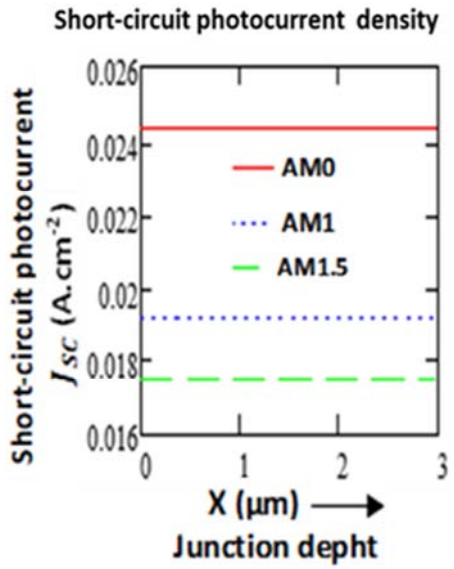

Figure 8. *Short-circuit photocurrent density vs. junction depth (x) under polychromatic illumination (AM0, AM1, AM1.5 solar spectra).*

It should be noted that the short-circuit photocurrent depends on the parameters considered. It varies by varying the values of certain parameters such as the diffusion length, the thickness and the recombination velocity. The Optimization of parameters during growth of materials is essential to obtain better photocurrent.

3.2. Study of Intrinsic Basic Parameters Under AM0, AM1 and AM1.5 Spectra

In this part we study the behavior of the structure for three reference solar spectra. We maintain the parameters used in Table 1. A relation similar to the expression (36) allows to obtain, the graphs of the generation rate, of the densities of minority carriers and the densities of photocurrent versus junction depth under AM0, AM1 and AM1.5 solar spectra.

We have:

$$S^*(x) = \int_1^4 S\,(E,x)dE \approx \frac{\delta E}{2}[S(E_1,x) + S(E_{m+1},x) + 2\sum_{i=2}^{m} S(E_i,x)] \quad (37)$$

$S(E,x)$ represents parameters such as generation rate, minority carrier density and photocurrent density.

3.2.1. Generation Rate

In Figure 9 we represent under AM0, AM1 and AM1.5 solar spectra the graph of the generation rate of carries (electrons and holes) versus junction depth. The generation rate shows three peaks modeling the absorptions of CdS (peak G_{R2-SCR}), $CuInS_2$ (peak G_{B-SCR}) and $CuInSe_2$ (peak G_{Sub}). ZnO layer absorbs above 3.1 eV, in this range (E. 3 eV) the incident photon flux is weak under the different solar spectra (AM0, AM1 and AM1.5) and explains why the absorption peak of ZnO does not appear. The low absorption of photons by the CdS layer is due to the low flux of incident photons above 2.5 eV for the different solar spectra. The absorption of the solar spectrum by the different regions of the cell is visible in the generation rate graph, this shows that the photons reach the different regions of the solar cell. However, we note also a low penetration depth of the photons (less than 3 um) due to the high photonic absorption coefficients of the used materials ($CuInSe_2$ and $CuInS_2$).

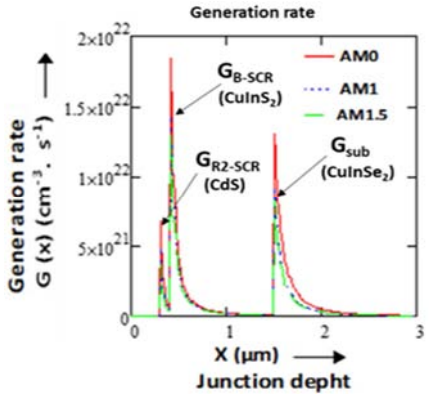

Figure 9. *Generation rate vs. junction depth (x) under polychromatic illumination (AM0, AM1, AM1.5 solar spectra).*

3.2.2. Minority Carrier Densities

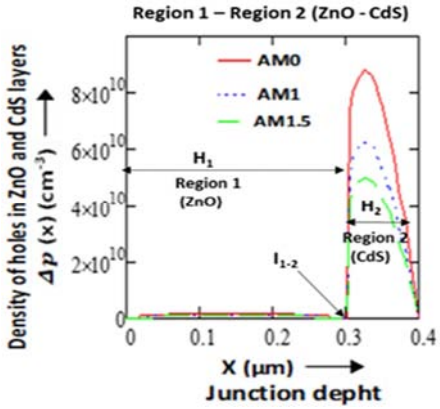

Figure 10. *Density of minority carriers photocreated vs. junction depth (x) under polychromatic illumination (AM0, AM1, AM1.5 solar spectra): density of holes in regions 1 and 2 (ZnO-CdS).*

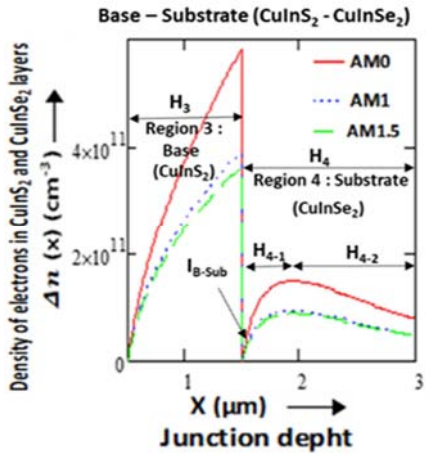

Figure 11. *Density of minority carriers photocreated vs. junction depth (x) under polychromatic illumination (AM0, AM1, AM1.5 solar spectra): density of electrons in regions 3 and 4 (base and substrate: $CuInS_2$ – $CuInSe_2$).*

Figure 10 shows the density of holes in ZnO (part H_1) and CdS (part H_2) layers, they are only generated in the CdS layer (part H_2). In n-doped ZnO and CdS, the holes are called minority carriers and participate in the photocurrent delivered by the solar cell when they reach the space charge region. This curve presents a maximum point in the vicinity of the interface, the diffusion of the generated carriers takes place from the maximum density point. The low ascending phase of this curve corresponds to a diffusion of the photo-generated holes towards the ZnO/CdS interface, these carriers are all lost by recombination phenomenon. The decreasing phase of the curve in this same region corresponds to a diffusion of the holes towards the space charge region, only the carriers which have sufficient diffusion length reach this latter and can participate to the photocurrent.

In Figure 11 we represent the density of electrons in the base ($CuInS_2$ layer: part H_3) and the substrate ($CuInSe_2$ layer: part H_4). In the p-doped base ($CuInS_2$) and substrate ($CuInSe_2$), electrons are the minority carriers and those that reach the space charge zone participate in the photocurrent delivered by the cell. In the substrate, the generated electrons also have maximum density point, this point models two diffusion areas. The electrons diffuse on the one hand towards the base-substrate interface I_{B-Sub} (part H_{4-1}) where some will be collected in the base. Some may be lost by recombination either in bulk before reaching the interface or at the interface due to the presence of defects or dislocations which constitute recombination centers. On the other hand others electrons diffuse towards the back surface (part H_{4-2}) where they will be lost by recombination phenomenon in bulk and surface.

The density of generated electrons in the base is greater than those generated in the substrate. This is because the carriers reach the base before being absorbed by the substrate and the generation rate is higher in the base (peak G_{B-SCR}). In the base (part H_3), the electron density increases with the thickness, modeling the diffusion of carriers towards the space charge region and those wich have sufficient diffusion length ($L_{n_3} > H_3$) participate to the photocurrent supplied by the cell.

3.2.3. Resulting Photocurrent Densities of Minority Carriers

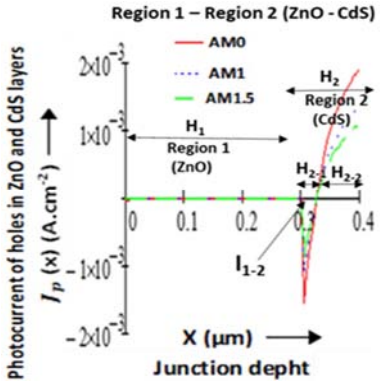

Figure 12. *Photocurrent density of minority carriers photocreated vs. junction depth (x) under polychromatic illumination (AM0, AM1, AM1.5 solar spectra): photocurrent density of holes in regions 1 and 2 (ZnO-CdS).*

Figure 12 shows the photocurrent density of holes in ZnO and CdS layers. In the ZnO layer (part H_1) there is no hole photocurrent because no carrier is generated in this region. In the CdS layer (part H_2) the generated carriers cause a negative hole photocurrent near the ZnO/CdS interface I_{1-2} (part H_{2-1}) and models photocurrent losses at the interface ($S_{p_2} = 2 \times 10^5$ cm.s^{-1}), the positive hole photocurrent models hole diffusion to the space charge region (part H_{2-2}). The negative part of the photocurrent explains the low ascending phase of hole density in the CdS layer and the positive part of the photocurrent explains the decreasing phase of the hole density in the CdS as illustrated in paragraph 3.2.2.

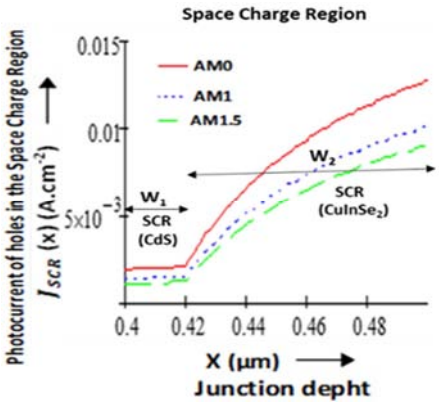

Figure 13. *Photocurrent density of minority carriers photocreated vs. junction depth (x) under polychromatic illumination (AM0, AM1, AM1.5 solar spectra).*

Figure 13 shows the photocurrent of holes in the space charge region. The space charge zone is formed by a part of the CdS layer and a part of the $CuInS_2$ layer. In the area W_1 formed only by CdS the photocurrent is almost constant for each solar spectrum, this behavior illustrates that the flux of photons absorbed by the CdS layer does not reach the space charge region. In the area W_2 formed only by $CuInS_2$ the photocurrent density increases with the thickness, this increase is due to the absorption of photons by this layer, the carriers generated in this area are supposed to be collected and participate directly in the photocurrent because of the high electric field which reigns in this region.

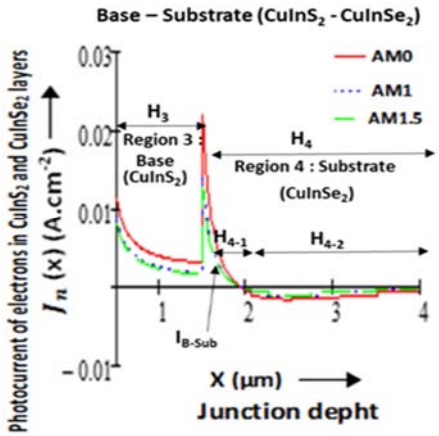

Figure 14. *Photocurrent density of minority carriers photocreated vs. junction depth (x) under polychromatic illumination (AM0, AM1, AM1.5 solar spectra): photocurrent density of electrons in regions 3 and 4 (base and substrate: $CuInS_2 – CuInSe_2$).*

Figure 14 illustrates the photocurrent density of electrons in the rear areas (base and substrate: $CuInS_2$ and $CuInSe_2$). In the base ($CuInS_2$: part H_3) the photocurrent density of electrons is positive and increases near the collection area (space charge region). This is explained by the increase of the electron density with the penetration depth of photons in this area as illustrated in the previous paragraph. In the substrate ($CuInSe_2$: part H_4) we observe photocurrent losses (part H_{4-2}). In the part where the current of electrons is positive (part H_{4-1}), the electrons diffuse towards the base-substrate interface I_{B-Sub} and the photocurrent increases considerably. At the interface (I_{B-Sub}) the carrier losses by recombination ($S_{n_3} = 2 \times 10^5$ cm.s^{-1}) reduce the electron photocurrent collected in the base.

3.2.4. Photocurrent Densities Through the Whole Structure

The short-circuit photocurrent is the sum of the electron and hole currents collected, it is constant and is shown in table 2 and figure 8. This current depends primarily on the carriers passing through the space charge zone. Since the short-circuit photocurrent is constant, we can determine the current of majority carriers in each region. This allows to draw the currents of electrons and holes through the whole structure.

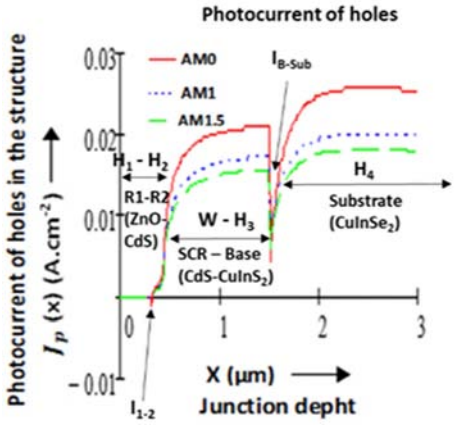

Figure 15. *Photocurrent density of carriers vs. junction depth (x) under polychromatic illumination (AM0, AM1, AM1.5 solar spectra throughout the structure: photocurrent density of holes.*

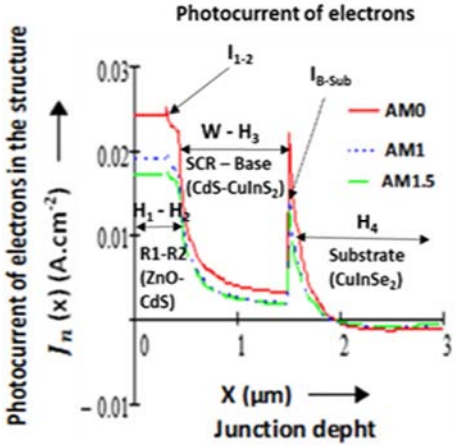

Figure 16. *Photocurrent density of carriers vs. junction depth (x) under polychromatic illumination (AM0, AM1, AM1.5 solar spectra throughout the structure: photocurrent density of electrons.*

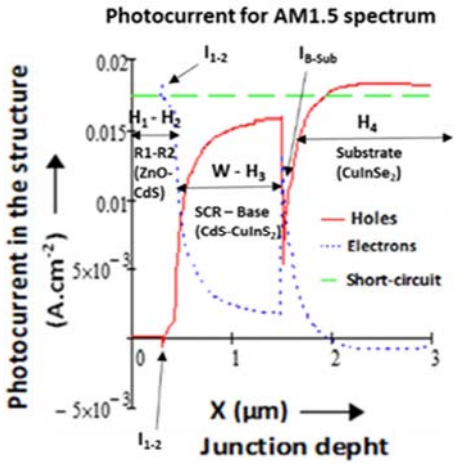

Figure 17. *Photocurrent density of carriers vs. junction depth (x) under polychromatic illumination (AM0, AM1, AM1.5 solar spectra throughout the structure: electron, hole and short-circuit photocurrents vs. junction depth (x) under polychromatic illumination throughout the structure for AM1.5 solar spectrum.*

In figures 15 and 16, we represent respectively the profiles of the hole and electron photocurrents in the different regions of the solar cell structure for the various solar spectra used (AM0, AM1 and AM1.5). In figure 17 we have represented on the same graph the photocurrents of electrons and holes, and the resulting short-circuit photocurrent for AM1.5 spectrum.

In each graph, the part $H_1 - H_2$ shows the behavior of photocurrent (electrons or holes) in ZnO and CdS layers, the part $W - H_3$ shows its behavior in the space charge region and the base, and the part H_4 shows its behavior in the substrate. At the ZnO/Cds interface the photocurrent is modeled by the peak I_{1-2}, and at the $CuInS_2/CuInSe_2$ interface by the peak I_{B-Sub}.

4. Conclusion

In this work a method of determining the short-circuit photocurrent for a given solar spectrum (AM0, AM1 and AM1.5) was illustrated from the model $ZnO(n^+)/CdS(n)/CuInS_2(p)/CuInSe_2$ (p^+) (model $n^+/n/p/p^+$). This method is based on the continuity equation of charge carriers and on the electrical, structural and optical properties of materials characterized by certain parameters and the imposed boundary conditions that take into account phenomena or states of the interface. Newton's quadrature is used to determine the short-circuit photocurrent for the three solar spectra and the results obtained (24.52 mA.cm^{-2} for AM0, 19.30 mA.cm^{-2} for AM1, 17.50 mA.cm^{-2} for AM1.5) with the considered parameters are well within the range obtained experimentally in the literature.

Subsequently, using the same principle of calculation under polychromatic illumination, we represented and analyzed the profiles of certain intrinsic parameters, namely the generation rate, the hole and electron densities and the corresponding current densities. These studies have shown a low penetration depth of the absorbed photons less than 3 µm due to the high absorption coefficients of the materials used in the solar

spectrum. This study also highlighted the direction of diffusion of electrons and holes and the location of carrier losses. These losses are due to surface and interface effects, material purity and the effect of carrier generation and diffusion.

This study presents a method of determining the short-circuit photocurrent from a solar spectrum and highlights the importance of optimizing the growth of materials and a proper dimensioning of layers for better collection of charge carriers.

As recommendations, we suggest the study of the response of the cell with optimized variations of the values of the various parameters (thickness of layers, diffusion length, recombination velocity, etc…) to evaluate the limit performance of this model. A similar study by inverting the layers of $CuInse_2$ and $CuInS_2$ leads to a no decreasing band gap structure and would be also interesting to study for the determination and the optimization of the short-circuit photocurrent. This calculation model is applicable to several types of structure (ZnO/CdS/CIGS, ZnO/CdS/CdTe, ZnO/CdS/CZTS, etc…) to model charge carriers transport in solar cell devices.

Nomenclature

Layer i: Region 1 ZnO (n^+), Region 2 CdS (n), Region 3 $CuInS_2$ (p), Region 4 $CuInSe_2$ (p^+)

Minority carriers: Holes (p), Electrons (n)

Absorption coefficient (cm^{-1}): α_i

Diffusion coefficient $(cm^2.s^{-1})$: D_{p_i}, D_{n_i}

Lifetime (μs): τ_{p_i}, τ_{n_i}

Diffusion length (μm): L_{p_i}, L_{n_i}

Mobility $(cm^2.V^{-1}.s^{-1})$: μ_{p_i}, μ_{n_i}

Recombination velocity (surface or interface) $(cm.s^{-1})$: S_{p_i}, S_{n_i}

Density (electrons or holes) (cm^{-3}): Δp_i, Δn_i

Photocurrent density (electrons or holes$(A.cm^{-2})$: J_{p_i}, J_{n_i}

Thickness (μm): H_i

Generatioon rate $(cm^{-3}.s^{-1})$: G_i

Φ: Incident photon flux $(cm^{-2}.s^{-1}.\mu m^{-1})$

F: Incident photon flux $(cm^{-2}.s^{-1}.eV^{-1})$

R: Reflection coefficient of region 1 (ZnO)

J_{ph}: Total density of photocurrent $(A.cm^{-2}.eV^{-1})$

J_{sc}: Short-circuit photocurrent density $(A.cm^{-2})$

H: Thickness of the structure (μm)

w_1: Thickness of CdS layer in the space charge region (SCR) (μm)

w_2: Thickness of $CuInS_2$ layer in the space charge region (SCR) (μm)

w: Thickness of the space charge region (μm)

J_{w_1}: Photocurrent density of holes in CdS layer in the space charge region (SCR) $(A.cm^{-2})$

J_{w_2}: Photocurrent density of holes in $CuInS_2$ layer in the space charge region (SCR) $(A.cm^{-2})$

q: Elementary charge $(1.6 \times 10^{-19}C)$

References

[1] Subba Ramaiah Kodigala, "$Cu(In_{1-x}Ga_x)se_2$ based thin solar cells", 2010, Volume 35, Academic Press, ELSEVIER. Inc, p. 16. Heise, L., Greene, M., Opper, N., Stavropoulou, M., & Equality, N. A. (2019). Gender inequality and restrictive gender norms: framing the challenges to health. The Lancet, 393, 2440-2454.

[2] H. Hahn, G. Frank, W. Klinger, A. D. Meyer, G. Stroger, "Über einige ternäre Chalkogenide mit Chalcopyritestruktur", Z. Anorg. Aug. Chem. 271 (1953) 153.

[3] T. Loher, W. Jaegermann, C. Pettenkofer, "Formation and electronic properties of the $CdS/CuInSe_2$ (011) heterointerface studied by synchrotron-induced photoemission", J. Appl. Phys. 77 (1995) 731.

[4] E. M. Keita, B. Ndiaye, M. Dia, Y. Tabar, C. Sene, B. Mbow, "Theoretical Study of Spectral Responses of Heterojunctions Based on $CuInSe_2$ and $CuInS_2$" OAJ Materials and Devices, Vol 5#1, 0508 (2020) – DOI: 10.23647/ca.md20200508.

[5] H. L. Hwang, C. Y. Sun, C. Y. Leu, C. C. Cheng, C. C. Tu, "Growth of $CuInS_2$ and its characterization", Rev. Phys. Appl. 13 (1978) 745.

[6] M. Robbins, V. G. Lambrecht Jr., "Preparation and some properties of materials in systems of the type $M^IM^{III}S_2$ / $M^IM^{III}Se_2$ where M^I=Cu, Ag and M^{III}=Al, Ga, In", Mater. Res. Bull. 8 (1973) 703.

[7] I. V. Bodnar, B. V. Korzun, A. I. Lukomski, "Composition Dependence of the Band Gap of $CuInS_{2x}Se_{2(1-x)}$", Phys. Stat. Solidi (B) 105 (1981) K143.

[8] S. J. Fonash, Solar Cell device Physics, Academic Press, New York, 1981.

[9] E. M. Keita, B. Mbow, M. S. Mane, M. L. Sow, C. Sow, C. Sene "Theoretical Study of Spectral Responses ofHomojonctions Based on $CuInSe_2$" Journal of Materials Science & Surface Engineering, Vol. 4 (4), 2016, pp 392-399.

[10] Abazović Nadica D., Jovanović Dragana J., Stoiljković Milovan M., Mitrić Miodrag N., Ahrenkil Phillip S., Nedeljković Jovan M., Čomor Mirjana I., "Colloidal-chemistry based synthesis of quantized $CuInS_2/Se_2$ nanoparticles", Journal of the Serbian Chemical Society, 2012, Volume 77, Pages: 789-797.

[11] Hisashi Yoshikawa, Sadao Adachi, "Optical Constants of ZnO", Jpn. J. Appl. Phys. Vol 36 (1997) pp. 6237-6243.

[12] B. MBOW, A. MEZERREG, N. REZZOUG, and C. LLINARES, "Calculated and Measured Spectral Responses in Near-Infrared of III-V Photodetectors Based on Ga, In, and Sb", phys. Stat. Sol. (a) 141, 511 (1994).

[13] H. J. HOVEL and J. M. WOODALL, "$Ga_{1-x}Al_xAs$ - GaAs P-P-N Heterojunction Solar Cells", J. Electrochem. Soc. 120, 1246 (1973).

[14] H. J. HOVEL and J. M. WOODALL, 10th IEEE Photovoltaic Specialists Conf., Palo Alto (Calif.) 1973 (p. 25).

[15] Alain Ricaud, "Photopiles Solaires", de la physique de la conversion photovoltaïque aux filières, matériaux et procédés. 1997, 1e édition, Presses polytechniques et universitaires romandes, p. 40.